Constructing the nonclassical lifetime distribution of two-level systems via quantum reliability

Yaotian Li,[1] Y.-M. Du,[2,*] Wenkui Ding,[1,†] Zhaoyu Fei,[1] Libin Fu,[2] and Xiaoguang Wang[1,‡]
[1]*Zhejiang Key Laboratory of Quantum State Control and Optical Field Manipulation, Department of Physics, Zhejiang Sci-Tech University, 310018 Hangzhou, China*
[2]*Graduate School of China Academy of Engineering Physics, Beijing 100193, China*

(Received 8 June 2025; accepted 26 August 2025; published 25 September 2025; corrected 12 November 2025)

To characterize the aging process of quantum devices, the concept of quantum reliability has recently been proposed as a process-based metric that quantifies the duration during which operations remain unaffected by noise. This duration is referred to as the lifetime of a quantum system. In this paper, we investigate the lifetime of a two-level atomic system undergoing spontaneous emission. We construct an exact statistical ensemble of the lifetimes for two-level systems using quantum reliability theory, incorporating comprehensive information such as mean values, fluctuations, and non-classical properties. Notably, we demonstrate that the ensemble exhibits can be represented by a density matrix, which is recorded in the monitoring apparatus by an observation process. Under the Born-Markov approximation, the diagonal elements decay exponentially at a state-dependent rate related to quantum fidelity. Beyond this approximation, the off-diagonal elements arise from interference between radiation pathways and are determined by the first-order coherence of the field. This feature indicates that the off-diagonal elements encode spectral information beyond the Markovian decay rate, suggesting a potential protocol for probing the environmental spectral density using two-level atoms.

DOI: 10.1103/w98h-hqb2

I. INTRODUCTION

The aging process is omnipresent in nature, affecting not only living organisms but also artificial devices [1–5]. To quantify aging processes, reliability theory introduces the lifetime distribution as a central concept in traditional industry and engineering. These concepts have been extended to the quantum world [6–11], providing a framework to characterize the aging of recent quantum devices [11–15].

In quantum systems, the lifetime may be ambiguous because this quantity pertains to a process rather than being time-local. To illustrate this, consider the simplest quantum system, the two-level system: how long can it preserve its initial state or remain under control?

The quantum fidelity, an important concept in quantum physics, was first introduced by Uhlmann in 1976 [16]. It quantifies the distinguish ability between two quantum states, and its mathematical definition is not unique. Several alternative formulations of fidelity have been proposed and discussed [17–20]. However, the Uhlmann fidelity is the most widely adopted, as it is naturally related to the Bures distance [21–23]. The lifetime, as a characteristic quantity, can be defined via quantum fidelity as the reciprocal of its decay rate.

In quantum reliability theory, the lifetime is to characterize how long the system stays in the target state or undergoes a target evolution. In this purpose, a non-classical lifetime distribution ϱ is introduced to depict the difference between the real system and the ideal system, The measure of the cumulative function of lifetime distribution in quantum reliability is, in a sense, an extension of quantum fidelity. This relates closely to the recent issue of quantifying the time spans of quantum state varies, such as quantum first passage time [24,25], quantum tunneling time [26–30], time spans of quantum transitions [25,31], and so on.

To illustrate explicitly the properties of the lifetime distribution, we consider a two-level atom under dissipation. Firstly, to compare it with the process fidelity [23], we employ the Lindblad master equation [22] within the Born-Markov approximation to describe dissipation processes. We focus on the effect of the measurement sequence length (i.e., the number of measurement operations) on quantum reliability, which characterizes the difference between the actual evolution trajectory and the ideal one. Secondly, to show how quantum reliability can capture more information about interference, we construct the full lifetime ensemble beyond the Born-Markov approximation. This ensemble is represented by a density matrix whose diagonal elements resemble fidelity, while the off-diagonal elements are determined by the first-order coherence function [32] of radiation fields. In this treatment, the lifetime of an atom is no longer treated merely as a characteristic quantity; rather, it is regarded as a measurable quantity with both mean value and fluctuations. Finally, we demonstrate that the lifetime distribution captured by a sequence of joint measurements contains full information about the environmental spectral density—both on- and off-resonance. This differs significantly from the initial-state fidelity, which primarily reveals the spontaneous emission rate determined by the spectral density near the resonance

*Contact author: ymdu@gscaep.ac.cn
†Contact author: wenkuiding@zstu.edu.cn
‡Contact author: xgwang@zstu.edu.cn

frequency. These results are based on a single two-level system; many-body extensions are left for further investigation.

The rest of this work is organized as follows. In Sec. II, we study the Lindblad master equation for spontaneous atomic emission and, within the framework of consistent histories, analyze the quantum reliability of the atom as well as the coherence weights among different emission histories. We highlight the limitations of the Born-Markovian approximation in studying quantum reliability for two-level systems. In Sec. III A, we introduce the lifetime density matrix and interpret the physical significance of its elements. Then, we solve the atomic spontaneous emission process using the Weisskopf-Wigner approximation and present the corresponding lifetime density matrix. In Sec. III B, we examine a radiation field characterized by a power-law spectral density and specifically analyze the physical significance of the lifetime density matrix of two-level systems. In Sec. III C, we demonstrate that the off-diagonal elements of the density matrix can be obtained by observing delayed interference patterns, from which the spectral density of the environment can be derived. Finally, we conclude with a summary and discussion of the results in Sec. IV.

II. ANALYZE LIFETIME STATISTICS WITH MASTER EQUATION APPROACH

Consider an atom in radiation fields. The lifetime of the atomic excited state can be studied using the Markovian approximation. This is characterized by the timescale $1/\gamma$, where the spontaneous emission rate γ is determined by the spectral density of the radiation fields. Physically, this lifetime is not definite, since the atom may radiate at different times. Can this quantity be represented by a proper distribution? To answer this question, we construct the lifetime density matrix ϱ for the total atom–field system within the framework of quantum reliability theory.

In the theory of quantum reliability, an event representing survival is defined as a specific state at a discrete time point t_i and is associated with an orthogonal projector E_i. These projectors and $\mathbb{1} - E_i$ represent survival and failure events, respectively. A trajectory $\mathcal{Y}$ up to time t_f constitutes a sequence of events occurring at discrete time points $t_0 < t_1 < \cdots < t_f$, represented by

$$\mathcal{Y} = E_0 \to E_1 \to \cdots \to E_f. \tag{1}$$

For a closed quantum system described by a unitary operator $U(t', t)$, the probability weight for trajectories $\mathcal{Y}$ is defined as [33]

$$W[\mathcal{Y}, \mathcal{Y}, U] = \mathrm{Tr}\left[\prod_{i=0}^{f-1} \mathcal{P}_{(E_{i+1},E_{i+1})} \circ \mathcal{U}(t_{i+1}, t_i)(E_0)\right], \tag{2}$$

where two superoperators $\mathcal{U}$ and $\mathcal{P}_{(E_i,E_i)}$ are defined as

$$\mathcal{U}\rho = U\rho U^\dagger, \quad \mathcal{P}_{(E_i,E_i)}(\rho) = E_i \rho E_i^\dagger, \tag{3}$$

with ρ being an arbitrary operator.

Consider another sequence of events occurring at time points $t_0 < t_1 < \cdots < t_f$, denoted as

$$\mathcal{Y}' = E'_0 \to E'_1 \to \cdots \to E'_f. \tag{4}$$

For a closed quantum system governed by the unitary transformation $U(t', t)$, the coherence between trajectory $\mathcal{Y}'$ and trajectory $\mathcal{Y}$ is referred to as a coherent history, and the weight of this coherence is given by:

$$W[\mathcal{Y}, \mathcal{Y}', U] = \mathrm{Tr}\left[\prod_{i=0}^{f-1} \mathcal{P}_{(E_{i+1},E'_{i+1})} \circ \mathcal{U}(t_{i+1}, t_i)(E_0)\right]. \tag{5}$$

where the superoperator $\mathcal{P}_{(E_i,E'_i)}$ is defined as

$$\mathcal{P}_{(E_i,E'_i)}(\rho) = E_i \rho E_i'^\dagger,$$

with ρ being an arbitrary operator.

The diagonal elements ϱ_{NN} are defined as the probability that the system survives the first $N-1$ measurements and fails at the N-th measurement:

$$\varrho_{NN} = \mathrm{Tr}\Bigg[\mathcal{P}_{(E_N^\perp,E_N^\perp)} \circ \mathcal{U}(t_N, t_{N-1}) \times \prod_{i=0}^{N-2} \mathcal{P}_{(E_{i+1},E_{i+1})} \circ \mathcal{U}(t_{i+1}, t_i)(\rho_0)\Bigg], \tag{6}$$

where $E_i^\perp = \mathbb{1} - E_i$. The off-diagonal elements ϱ_{NM} with $N \neq M$ represent the quantum interference between two paths: one where the system fails at the N-th measurement and the other where it fails at the M-th measurement:

$$\begin{aligned}\varrho_{NM} = \mathrm{Tr}(&\mathbb{1}U_M(\delta t)\cdots E_N^\perp U_N(\delta t)E_{N-1}U_{N-1}(\delta t)\\ &\times \cdots E_1 U_1(\delta t)\,|\psi_0\rangle\\ &\langle\psi_0|\,U_1^\dagger(\delta t)E_1\cdots U_{M-1}^\dagger(\delta t)E_{M-1}U_M^\dagger(\delta t)E_M^\perp),\\ &N < M\end{aligned} \tag{7}$$

where the evolution operator $U_i(\delta t)$ describes evolution over the time interval from $(i-1)\delta t$ to $i\delta t$.

From the perspective of the real model, the diagonal elements of the matrix represent the probability distribution of photon emission times, and the off-diagonal elements capture the quantum interference between radiation fields emitted at different intervals. It can be seen that the matrix $\varrho = \sum_{NM} \varrho_{NM}|N\rangle\langle M|$ satisfies the following properties: (i) $\mathrm{Tr}(\varrho) = 1$, (ii) $\varrho^\dagger = \varrho$, and (iii) $X^T \varrho X \geqslant 0$, for all complex vectors X. Therefore, we refer to ϱ as the lifetime density matrix. It was shown [6] that this density matrix corresponds to the monitor's final state after the time-sequence measurement, and that $|N\rangle$ forms its measurement basis. We illustrate the origin of the off-diagonal terms in Fig. 1, which depicts the interference between radiation fields emitted at two distinct times.

Consider the case where survival means the system remains in a specific state, with $E_0 = E_1 = E_2 = \cdots = |\psi_0\rangle\langle\psi_0|$. The diagonal elements define a classical distribution, whose cumulative form $R(N\delta t) = \sum_{M=(N+1)}^{\infty} \varrho_{MM}$ represents the probability that the system survives up to N steps, and is given by

$$R(N\delta t) = \langle\psi_0|\,\rho(\delta t)\,|\psi_0\rangle^N. \tag{8}$$

The quantum fidelity between two density operators ρ_0 and ρ_1 is defined as [16,17]

$$F(\rho_0, \rho_1) = \mathrm{Tr}\sqrt{\sqrt{\rho_0}\rho_1\sqrt{\rho_0}}. \tag{9}$$

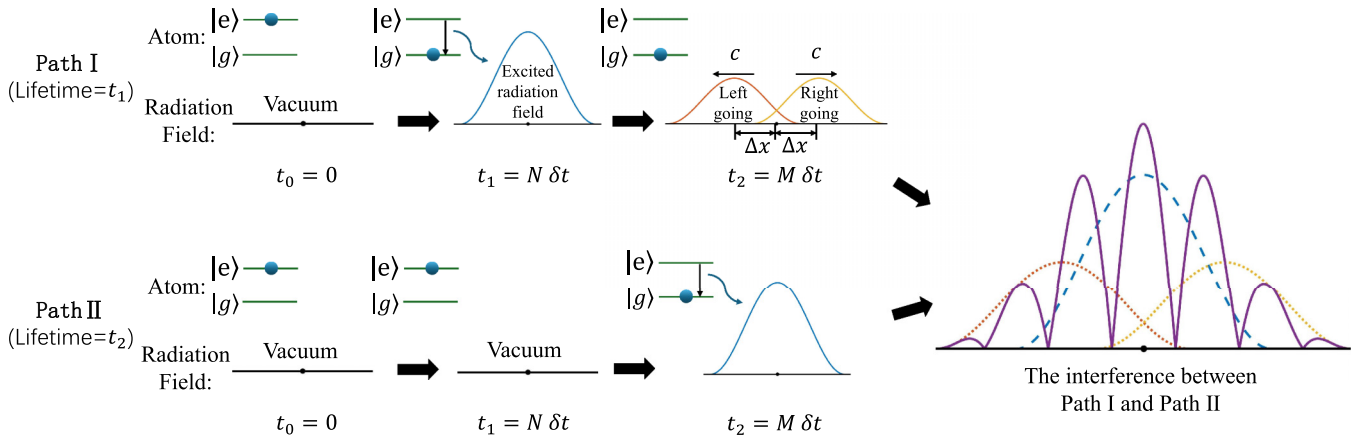

FIG. 1. Scheme to illustrate the picture of off-diagonals, i.e., interference between different paths. Path I presents that the atom emits at time $n\delta t$, and the radiation then splits and propagates along the positive and negative directions of x by a distance $\Delta x = c(m-n)\delta t$. Path II presents that the atom emits at time $m\delta t$. The rightmost image illustrates the interference between the excited radiation fields by the two emission events.

If one of the operators, for instance $\rho_0 = |\psi_0\rangle\langle\psi_0|$, is a pure state, then $\sqrt{\rho_0} = \rho_0$. Consequently, the fidelity simplifies to

$$F(\rho_0, \rho_1) = \sqrt{\langle\psi_0|\,\rho_1\,|\psi_0\rangle}. \tag{10}$$

It follows that quantum reliability can be expressed in terms of the fidelity as

$$R(N\delta t) = F[\rho(0), \rho(\delta t)]^{2N}. \tag{11}$$

In other words, the reliability equals the fidelity between the states at times 0 and δt raised to the $2N$-th power.

Next, we consider the general form of the Lindblad master equation

$$\dot{\rho} = -i[H, \rho] + \sum_{\mu=1}^{L} \mathcal{D}(c_\mu)\rho, \tag{12}$$

in which,

$$\mathcal{D}(c_\mu)\rho = c_\mu \rho c_\mu^\dagger - \tfrac{1}{2}\{c_\mu^\dagger c_\mu, \rho\}. \tag{13}$$

where, c_μ denotes the Lindblad operator associated with the μ-th decay channel.

Assuming the atom is initially in an excited state with zero photons in the field; then $c_\mu = \sqrt{\gamma}\sigma_-$, and the quantum reliability is given by

$$R(t) = e^{-\gamma t}. \tag{14}$$

Since the Born approximation neglects the field dynamics, the off-diagonal elements vanish:

$$\varrho_{NM} = 0. \tag{15}$$

(The detailed derivation is presented in Appendix A).

These results suggest that, for spontaneous emission from two-level atoms, quantum reliability and fidelity-based information exhibit very similar behavior under the Born–Markov approximation. The sole distinction is that quantum reliability partitions the evolution into discrete segments. In the following sections, we demonstrate that the two concepts diverge significantly once the Born–Markov approximation is relaxed.

III. ANALYZE LIFETIME STATISTICS BEYOND MARKOVIAN MASTER EQUATION

Because the off-diagonal elements of the lifetime density matrix for a two-level atomic system vanish under the Markov master equation, we employ the Weisskopf–Wigner approximation instead of the Born–Markov approximation to analyze this system and elucidate its physical significance. We then consider the full Hamiltonian describing the interaction between a single atom and a multimode optical field. By analyzing the resulting lifetime density matrix, we reveal the physical insights it provides.

A. Lifetime density matrix

We again assume the system remains in the excited state. The total Hamiltonian is given by

$$H = H_{\text{atom}} + H_{\text{field}} + H_{\text{int}}. \tag{16}$$

Here, the $H_{\text{atom}} = \omega_0\sigma_+\sigma_-$ is the atom's free Hamiltonian with resonance frequency ω_0; the second term $H_{\text{field}} = \sum_k \omega_k \hat{a}_k^\dagger \hat{a}_k$ is the free Hamiltonian of the radiation field, where $\hat{a}_k$ denotes the annihilation operator for the k-th mode of the radiation field; and H_{int} describes the atom–field interaction.

We proceed by making the rotating-wave approximation (RWA), and expressing the atom–field interaction Hamiltonian as follows:

$$H_{\text{int}} = \sum_k (g_k\sigma_+\hat{a}_k + \text{H.c.}), \tag{17}$$

where the g_k denotes the atom–field coupling strength.

Assuming the system is initially in the excited state and the radiation field is in the vacuum state, the total state at time $t > 0$ can be written as

$$|\psi(t)\rangle = b(t)\sigma_+\,|g, 0\rangle + \sum_k c_k(t)\hat{a}_k^\dagger\,|g, 0\rangle\,, \tag{18}$$

where $b(t)$ and $c_k(t)$ are the probability amplitudes for the atomic excitation and the photon in mode k,respectively. Moreover, $|g, 0\rangle$ denotes the combined ground state, with $|g\rangle$

the atomic ground state and $|0\rangle$ the field vacuum state. From the Schrödinger equation, the time evolution of $b(t)$ and $c_k(t)$ obeys

$$\dot{b}(t) = -\mathrm{i}\sum_k g_k c_k(t) - \mathrm{i}\omega_0 b(t),$$
$$\dot{c}_k(t) = -\mathrm{i}g_k^* b(t) - \mathrm{i}\omega_k c_k(t). \tag{19}$$

Assuming that the initial state is $|\psi_0\rangle = |e,0\rangle$. By applying the Weisskopf–Wigner approximation, the solution becomes

$$b(t) = e^{-\mathrm{i}\omega_0 t - \frac{\gamma t}{2}},$$
$$c_k(t) = -\mathrm{i}g_k^* \frac{e^{-\mathrm{i}\omega_0 t - \frac{\gamma t}{2}} - e^{-\mathrm{i}\omega_k t}}{\mathrm{i}(\omega_k - \omega_0) - \frac{\gamma}{2}}. \tag{20}$$

where, the Lamb shift is neglected, and the dissipation rate γ is given by

$$\frac{\gamma}{2} = \mathrm{Re}\int_0^\infty \sum_k |g_k|^2 e^{-\mathrm{i}(\omega_k-\omega_0)\tau}\mathrm{d}\tau. \tag{21}$$

This leads to Fermi's golden rule $\gamma = 2\pi J(\omega_0)$, where the spectral density $J(\omega)$ is defined as

$$J(\omega) = \sum_k |g_k|^2 \delta(\omega - \omega_k). \tag{22}$$

Then, the lifetime density matrix can be expressed as:

$$\begin{aligned}\varrho_{NM} &= \mathrm{Tr}(\mathbb{1}U'(\delta t)\cdots E_0^\perp U(\delta t)E_0 U(\delta t)\cdots E_0 U(\delta t)\,|\psi_0\rangle \\ &\quad \langle\psi_0|\,U^\dagger(\delta t)E_0\cdots U^\dagger(\delta t)E_0 U^\dagger(\delta t)E_0^\perp) \\ &= \langle\psi_0|\,U(\delta t)\,|\psi_0\rangle^{N-1}\,\langle\psi_0|\,U^\dagger(\delta t)\,|\psi_0\rangle^{M-1} \\ &\quad \times \langle\psi_0|\,U^\dagger(\delta t)E_0^\perp U((M-N)\delta t)E_0^\perp U(\delta t)\,|\psi_0\rangle \end{aligned} \tag{23}$$

where $E_0 = |\psi_0\rangle\langle\psi_0|$. And we define an overlap function as

$$T_{\delta t}((M-N)\delta t) = \frac{\varrho_{NM}}{\sqrt{R((N-1)\delta t)R((M-1)\delta t)}}. \tag{24}$$

To reveal their physical meaning, we further neglect the reabsorption process, yielding

$$\begin{aligned}\varrho_{NM} &\approx b^{(N-1)}(\delta t)b^{*(M-1)}(\delta t) \\ &\quad \times \int_{-\infty}^{\infty} G_{\delta t}^{(1)}(x,x;(M-N)\delta t,0)\mathrm{d}x \\ &= e^{-\frac{\gamma\delta t(M+N-2)}{2}} e^{-\mathrm{i}\omega_0\delta t(N-M)} \int_0^\infty J(\omega)e^{-\mathrm{i}\omega(M-N)\delta t} \\ &\quad \times \frac{(e^{-\gamma\delta t} - 2e^{-\frac{\gamma\delta t}{2}}\cos((\omega-\omega_0)\delta t)+1)}{\frac{\gamma^2}{4}+(\omega-\omega_0)^2}\mathrm{d}\omega. \end{aligned} \tag{25}$$

These off-diagonal elements represent interference between radiation fields across the entire spatial domain. This equation shows that the off-diagonal elements can be expressed in terms of the first-order coherence function, $G_{\delta t}^{(1)}(x,x';t,0) \equiv \langle\psi(\delta t)|\mathcal{E}^{(-)}(x,t)\mathcal{E}^{(+)}(x',0)|\psi(\delta t)\rangle$, where $\mathcal{E}^{(\pm)}(x,t)$ denote the annihilation (creation) operators of the radiation field at the space-time point (x,t), and $|\psi(\delta t)\rangle = U(\delta t)|\psi_0\rangle$ (see Appendix B for details). Thus, the off-diagonal terms are determined by the spectral density of the radiation field.

The off-diagonal element ϱ_{NM} represents interference between field excitations at times $N\delta t$ and $M\delta t$ over the entire spatial domain. This interference is directly determined by the time interval between the two emission events. The exponential factor $\exp[-\gamma\delta t(M+N-2)/2]$ governs the interference strength. For a fixed difference $M-N$, larger values of M and N correspond to weaker interference. Due to time-translation symmetry, the remaining part depends only on the time difference and is denoted by the value of the overlap function $T_{\delta t}((M-N)\delta t)$, defined as

$$\begin{aligned}T_{\delta t}\big((M-N)\delta t\big) &\approx e^{-\mathrm{i}\omega_0\delta t(N-M)} \\ &\quad \times \int_{-\infty}^{\infty} G_{\delta t}^{(1)}(x,x;(M-N)\delta t,0)\mathrm{d}x. \end{aligned} \tag{26}$$

Next, we consider the continuous limit $\delta t \to 0$ and fix $N\delta t = t, M\delta t = t'$. In this limit, the lifetime density matrix takes the form $\sum_{N,M}\varrho_{NM}|N\rangle\langle M| \to \int_0^\infty \mathrm{d}t\int_0^\infty \mathrm{d}t'\varrho(t,t')|t\rangle\langle t'|$, with

$$\begin{aligned}\varrho(t,t') &= e^{-\mathrm{i}\omega_0 t - \frac{\gamma t}{2} + \mathrm{i}\omega_0 t' - \frac{\gamma t'}{2}} \int_0^\infty J(\omega)e^{\mathrm{i}\omega(t-t')}\mathrm{d}\omega \\ &= \sqrt{R(t)R(t')}e^{-\mathrm{i}\omega_0(t-t')}\int_0^\infty J(\omega)e^{\mathrm{i}\omega(t-t')}\mathrm{d}\omega, \end{aligned} \tag{27}$$

where the cumulate function $R(t) \equiv \int_t^\infty \varrho(t',t')\mathrm{d}t'$.

B. Atomic lifetime density matrix in Ohmic spectral density

In this section, we focus on the Ohmic-type spectral density. We show that these matrix elements correspond to the coherence function of the radiation field. Specifically, we consider the Ohmic spectral density for the radiation field, although this property of the off-diagonal elements does not depend on the specific form of the spectral density.

The Ohmic-type spectral density is given as

$$J(\omega) = \eta\omega_c^{1-s}\omega^s \mathrm{e}^{-\frac{\omega}{\omega_c}}\Theta(\omega), \tag{28}$$

where η is a dimensionless constant, and ω_c is the cutoff frequency. The exponent s characterizes the environment as super-Ohmic ($s>1$), Ohmic ($s=1$), or sub-Ohmic ($s<1$). We set $\omega_c \gg \omega_0$ in the following analysis to ensure that sideband effects can be neglected.

The diagonal elements are simplified as

$$\varrho_{NN} = e^{-(N-1)\gamma\delta t}(1-e^{-\gamma\delta t}), \tag{29}$$

From Eq. (29), the atom's lifetime exhibits an exponential decay, with the emission rate given by $\gamma = 2\pi J(\omega_0)$. This result coincides with the prediction from the Born-Markov approximation.

We demonstrate in Fig. 2(a) the overlap between radiation fields emitted at different times. As shown in the figure, the field excited in the first interval ($N=1$, red curve) propagates in both directions and overlaps with the field excited in the interval ($M=2$). This non-vanishing overlap indicates that the corresponding off-diagonal elements of the lifetime density matrix are non-zero.

In Fig. 2(b), we illustrate the effect of the time delay τ between different emission intervals on the absolute value of the $T_{\delta t}((M-N)\delta t)$ for different values of s. This quantity depicts the overlap between the fields excited in time difference $|M-N|\delta t$. It is observed that $T_{\delta t}((M-N)\delta t)$ is

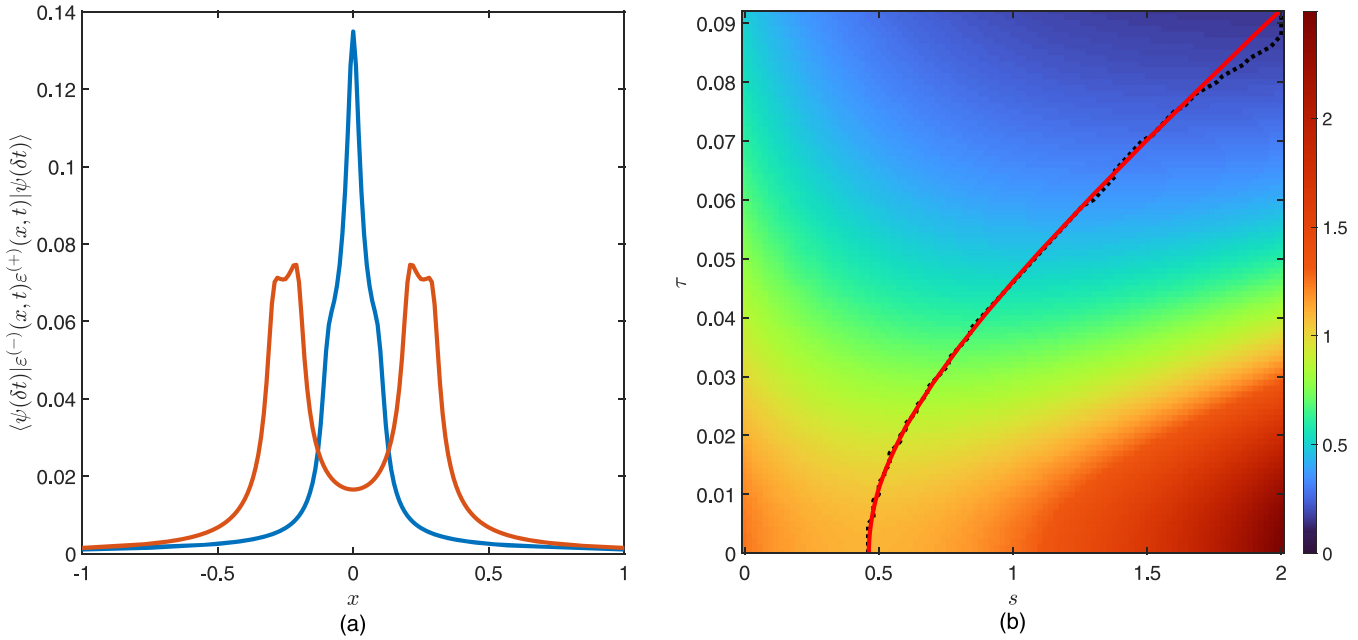

FIG. 2. (a) Radiation field interference of the atomic emission fields corresponding to the paths $N = 1$ and $M = 2$ with $\omega_c = 25$, $\omega_0 = 1$, $\delta t = 0.1$, $\eta = 0.002$, and the speed of light is $c = 1$, the upper cutoff frequency chosen as $\omega_d = 250$ under the sub-Ohmic spectral density ($s = 0.5$). The blue line represents the radiation field excited at time $N\delta t$, and the red line corresponds to the radiation field excited at time $M\delta t$. (b) The absolute value of the overlap $|T_{\delta t}((M-N)\delta t)|/(\delta t)^2$ varies with the Ohmic spectrum exponent s and the time interval $\tau = |M-N|\delta t$ between two paths, with $\omega_c = 25$, $\omega_0 = 1$, $\delta t = 0.001$, $\eta = 0.002$. And in the numerical simulations, the frequency integral is truncated at an upper limit of $\omega_d = 250$, with a discretization step of $\Delta\omega = 0.2$. The red (dashed) line indicates the exact (simulated) value of s for each τ to give the minimum of $|T_{\delta t}(\tau)|/(\delta t)^2$.

non-monotonic with s, i.e., with fixed $|M-N|$ there is minimum for the overlap that is achieved by some particular s.

Following with Eq. (27), the minimum value of the overlap occurs at

$$\partial_s|T_0(\tau)| = \eta\left(\tau^2 + \tfrac{1}{\omega_c^2}\right)^{-\frac{s+1}{2}}\omega^{1-s}\Gamma(1+s) \left[\Psi(0,1+s) - \tfrac{1}{2}\ln\left(\omega_c^2\tau^2+1\right)\right] = 0. \quad (30)$$

where $\tau = |M-N|\delta t$, $\Gamma(1+s)$ indicates the Gamma function, while $\Psi(0,1+s)$ stands for the Polygamma function. This non-monotonic behavior highlights the subtle influence of the spectral density exponent s on quantum coherence at short timescales.

To validate the approximations made in our analysis, we further perform numerical simulations of the system's

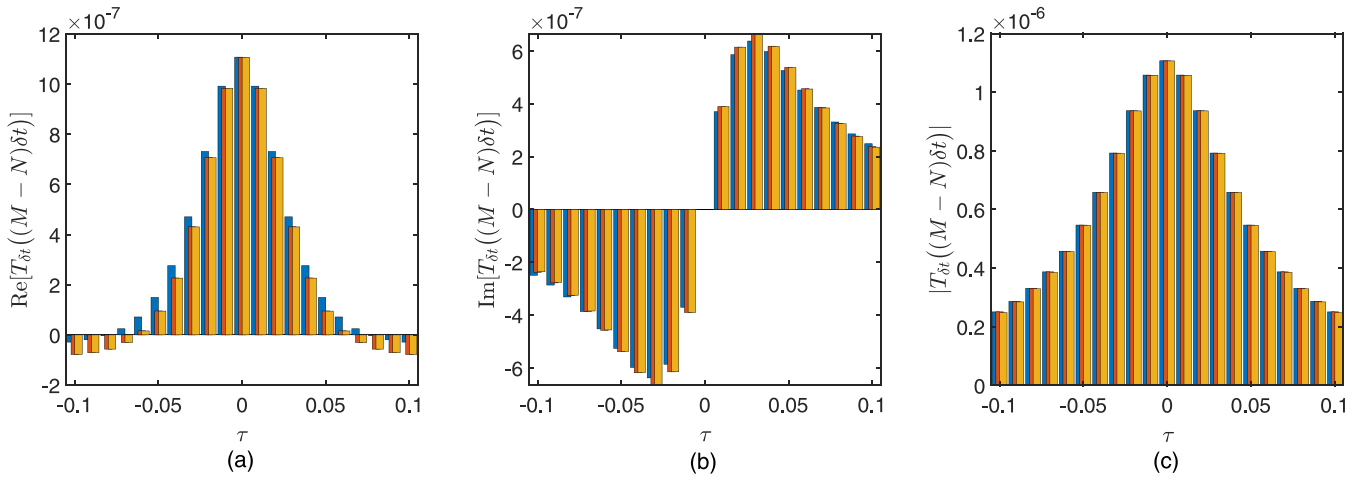

FIG. 3. Image of $T_{\delta t}((M-N)\delta t)$, the yellow bars present the simulated results, the red bars represent results that neglecting the reabsorption and the blue bars present the result neglecting the reabsorption and considering Weisskopf-Wigner approximation: (a) real part, (b) imaginary part, and (c) absolute value. In these numerical calculation, we choose the sub-Ohmic spectrum with $s = 0.5$, $\omega_c = 25$, $\omega_0 = 1$, $\eta = 0.002$ $\delta t = 0.001$. And in the numerical simulations, the frequency integral is truncated at an upper limit of $\omega_d = 250$, with a discretization step of $\Delta\omega = 0.2$.

evolution. Specifically, we present three sets of results: (i) the full simulation, (ii) the result obtained by neglecting reabsorption, and (iii) the result under the Weisskopf-Wigner approximation. The corresponding values of $T_{\delta t}((M-N)\delta t)$ for each case are plotted in Fig. 3. This comparison illustrates the discrepancies introduced by each approximation and provides insight into their respective accuracies.

C. Estimate spectral density via lifetime density matrix

The connection between the lifetime density matrix and the spectral density suggests that the former can be utilized for quantum bath spectral estimation. To briefly illustrate this idea, we recall Eq. (27).

If the lifetime density matrix is fully measured, the spectral density of the bath can be reconstructed from the data via

$$J(\omega)=\frac{1}{2\pi}\int_0^\infty \frac{\varrho(\tau,0)e^{\mathrm{i}(\omega_0-\omega)\tau}+\varrho(0,\tau)e^{\mathrm{i}(\omega-\omega_0)\tau}}{\sqrt{R(\tau)}}\mathrm{d}\tau. \tag{31}$$

This equation shows that lifetime distribution captures full information of the environmental spectral density, since to access the lifetime distribution requires a joint measurement on the system state at a sequence of time points [6]. Therefore, it provides more information than the fidelity, which capture the spectral density near the resonance frequency. This suggests a potential approach to probe the spectral density of the environment by measuring the lifetime distribution of the atom in the Markovian regime.

We simulate the measurement results and apply Eq. (31) to estimate the spectral density. In Fig. 4, we present a comparison between the original spectral density used in the simulation and the one reconstructed from the lifetime density matrix obtained by measuring atomic lifetimes. Different sampling intervals δt are considered.

From Fig. 4, we observe that when the sampling interval δt is too large, the low sampling resolution introduces significant errors in the estimation, as illustrated by the red curve. Conversely, when δt is too small, the Zeno effect suppresses the off-diagonal elements, leading to a failure in extracting meaningful interference information, as shown by the yellow curve. However, for a properly chosen sampling interval—small enough compared to $1/\gamma$, yet not too small relative to $1/\omega_c$ to avoid the Zeno effect—the reconstructed data (blue curve) closely match the original spectral density.

These results demonstrate that the quantum reliability framework provides a viable method for extracting information about system correlation functions and the spectral density of the environment.

.

IV. CONCLUSIONS AND DISCUSSIONS

In this paper, we applied the framework of quantum reliability to the lifetime distribution of two-level systems under spontaneous emission. We demonstrate that the resulting ensemble can be represented by a density matrix with a clear physical interpretation: its diagonal elements exhibit exponential decay determined by the initial state, while the off-diagonal elements capture interference between distinct

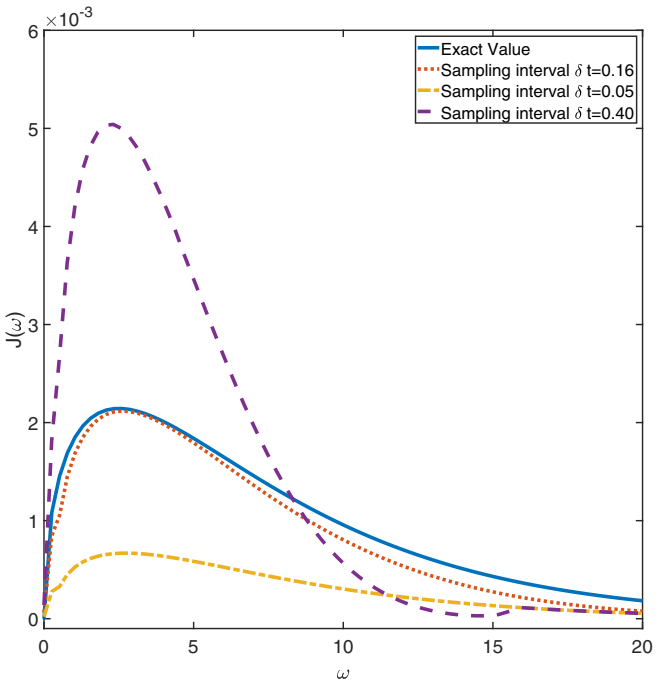

FIG. 4. Spectral density estimation, where the spectrum is Ohmic with $s=0.5$, and other parameters are set as $\omega_c=5$, $\omega_0=0.1$, $\eta=0.001$. And in the numerical simulations, the frequency integral is truncated at an upper limit of $\omega_d=20$, with a discretization step of $\Delta\omega=0.10$. In the estimation, we have used the discrete Fourier transformation.

emission events. Specifically, we derive an explicit relation between the lifetime density matrix and the spectral density of the radiation field. Given that the lifetime density matrix is experimentally accessible, this relation offers a potential method for estimating the spectral density in the Markovian regime. These results imply that quantum reliability, as an extension of fidelity, provides more comprehensive information by capturing the full spectral density of the two-level system.

In quantum theory, quantifying the time span of a quantum transition is a fundamental issue. This topic has been addressed in various contexts, with different definitions proposed to characterize temporal aspects of quantum systems. In contrast, quantum reliability offers an alternative approach by treating the time span as an observable determined by the measurement outcomes of the quantum system. This method not only explicitly describes the mean value but also captures fluctuations and quantum properties. Our further investigation aims to extend beyond the two-level system and explore the time–energy uncertainty relation [34,35], which can be accessed via different measurement protocols in open quantum systems.

ACKNOWLEDGMENTS

This work was supported by the Science Challenge Project (Grant No. TZ2025017), the Innovation Program for Quantum Science and Technology (Grant No. 2024ZD0301000), the Hangzhou Joint Fund of the Zhejiang Provincial Natural Science Foundation of China under Grant No.

LHZSD24A050001, the Science Foundation of Zhejiang Sci-Tech University (Grants No. 23062088-Y, No. 23062181-Y and No. 23062153-Y), the National Natural Science Foundation of China (Grants No. 12405046, No. 12305031 and No. 12088101), and the NSAF Grant No. U2330401.

DATA AVAILABILITY

The data that support the findings of this article are openly available [36].

APPENDIX A: QUANTUM RELIABILITY AND COHERENT HISTORIES OF SPONTANEOUSLY RADIATING ATOMS UNDER THE LINDBLAD MASTER EQUATION

For a general form of the Lindblad master equation

$$\dot{\rho} = -\mathrm{i}[H,\rho] + \sum_{\mu=1}^{L} \mathcal{D}(c_\mu)\rho, \tag{A1}$$

The spontaneous emission of the atom is described using the Lindblad master equation

$$\begin{aligned}\dot{\rho}(t) &= \gamma_0(1-\bar{n})\mathcal{D}(\sigma_-)\rho + \gamma_0\bar{n}\mathcal{D}(\sigma_+)\rho \\ &= \alpha\mathcal{D}(\sigma_-)\rho + \beta\mathcal{D}(\sigma_+)\rho,\end{aligned} \tag{A2}$$

where γ_0 characterizes the decoherence strength and $\sigma_- = \sigma_+^\dagger = |\downarrow\rangle\langle\uparrow|$ with $|0\rangle$ and $|1\rangle$ being the up and down levels, respectively. The mean fermionic number $\bar{n}$ is given by $\bar{n} = 1/[\exp(\omega/T)+1]$ satisfying

$$0 \leqslant \bar{n} \leqslant 0.5, \tag{A3}$$

and it depends on the temperature T and the characteristic frequency ω of the fermionic environment. The two dynamical decoherence rates α and β satisfy

$$\alpha+\beta = \gamma_0, \quad \alpha-\beta = (1-2\bar{n})\gamma_0. \tag{A4}$$

Comparing Eqs. (13) and (A2), we have

$$c_1 = \sqrt{\gamma_0(1-\bar{n})}\sigma_-, \quad c_2 = \sqrt{\gamma_0\bar{n}}\sigma_+. \tag{A5}$$

To study the reliability under decoherence described by the master equation in Eq. (A2), we use three superoperators given by

$$\begin{aligned}\mathcal{J}_-\rho(t) &= \sigma_-\rho(t)\sigma_+, \\ \mathcal{J}_+\rho(t) &= \sigma_+\rho(t)\sigma_-, \\ \mathcal{J}_0\rho(t) &= \tfrac{1}{2}[\sigma_+\sigma_-\rho(t) + \rho(t)\sigma_+\sigma_- - \rho(t)].\end{aligned} \tag{A6}$$

One can verify that they satisfy the su(2) commutation relations $[\mathcal{J}_+,\mathcal{J}_-] = 2\mathcal{J}_0$, $[\mathcal{J}_0,\mathcal{J}_\pm] = \pm\mathcal{J}_\pm$. Then the master equation in terms of three superoperators is obtained as

$$\dot{\rho}(t) = [\beta\mathcal{J}_+ + \alpha\mathcal{J}_- + (\beta-\alpha)\mathcal{J}_0 - \tfrac{1}{2}(\alpha+\beta)]\rho(t). \tag{A7}$$

The formal solution immediately follows as

$$\rho(t) = \mathcal{V}(t)[\rho(0)] = e^{[\beta\mathcal{J}_+ + \alpha\mathcal{J}_- + (\beta-\alpha)\mathcal{J}_0 - \frac{1}{2}\gamma_0]t}\rho(0), \tag{A8}$$

where the notation γ_0 denotes the sum of the two dynamical rates $\gamma_0 = (\alpha+\beta)$, and $\mathcal{V}(t)$ is the decoherence evolution operator of the system. To solve the master equation, we need to decompose the following exponential operator

$$\mathcal{V}(t) = e^{(\alpha_+\mathcal{J}_+ + \alpha_-\mathcal{J}_- + \alpha_0\mathcal{J}_0)t}. \tag{A9}$$

Formaly, the operator $\mathcal{V}(t)$ is decomposed as

$$\mathcal{V}(t) = e^{f_+(t)\mathcal{J}_+}e^{f_0(t)\mathcal{J}_0}e^{f_-(t)\mathcal{J}_-}, \tag{A10}$$

where $f_+(t)$, $f_0(t)$, $f_-(t)$ are time dependent coefficients. Making derivative of $\mathcal{V}$ with respect to time and using the Baker-Hausdorff formula, we could get the following system of differential equations:

$$\begin{aligned}\dot{f}_+(t) - f_+(t)\dot{f}_0(t) - e^{-f_0(t)}f_+^2(t)\dot{f}_-(t) &= \alpha_+, \\ \dot{f}_0(t) + 2e^{-f_0(t)}f_+(t)\dot{f}_-(t) &= \alpha_0, \\ e^{-f_0(t)}\dot{f}_-(t) &= \alpha_-.\end{aligned} \tag{A11}$$

Time dependent coefficients $f_+(t)$ $f_0(t)$ $f_-(t)$ can be obtained by solving the differential equations as

$$\begin{aligned}f_+(t) &= \frac{2\alpha_+\sinh|\epsilon_0 t|}{2\epsilon_0\cosh|\epsilon_0 t| - \alpha_0\sinh|\epsilon_0 t|}, \\ f_-(t) &= \frac{2\alpha_-\sinh|\epsilon_0 t|}{2\epsilon_0\cosh|\epsilon_0 t| - \alpha_0\sinh|\epsilon_0 t|}, \\ f_0(t) &= 2\ln\frac{2\epsilon_0}{2\epsilon_0\cosh|\epsilon_0 t| - \alpha_0\sinh|\epsilon_0 t|},\end{aligned} \tag{A12}$$

where $\epsilon_0 = \sqrt{\alpha_0^2/4 + \alpha_+\alpha_-}$.

The formal solution of the master equation (A2) is given by

$$\begin{aligned}\rho(t) = \mathcal{V}(t)\rho_0 &= e^{[\beta\mathcal{J}_+ + \alpha\mathcal{J}_- + (\beta-\alpha)\mathcal{J}_0 - \frac{1}{2}\gamma_0]t}\rho(0) \\ &= e^{-\frac{1}{2}\gamma_0 t}e^{x_+\mathcal{J}_+}e^{(\ln x_0)\mathcal{J}_0}e^{x_-\mathcal{J}_-}\rho(0).\end{aligned} \tag{A13}$$

Direct application of Eq. (A12) leads to

$$\begin{aligned}x_+(t) &= \frac{\beta(e^{\frac{1}{2}\gamma_0 t} - e^{-\frac{1}{2}\gamma_0 t})}{\alpha e^{\frac{1}{2}\gamma_0 t} + \beta e^{-\frac{1}{2}\gamma_0 t}}, \\ x_-(t) &= \frac{\alpha(e^{\frac{1}{2}\gamma_0 t} - e^{-\frac{1}{2}\gamma_0 t})}{\alpha e^{\frac{1}{2}\gamma_0 t} + \beta e^{-\frac{1}{2}\gamma_0 t}}, \\ x_0(t) &= \left(\frac{\alpha e^{\frac{1}{2}\gamma_0 t} + \beta e^{-\frac{1}{2}\gamma_0 t}}{\alpha+\beta}\right)^2.\end{aligned} \tag{A14}$$

Due to $\mathcal{J}_-^2 = 0$, $\mathcal{J}_+^2 = 0$, and $[\mathcal{J}_+,\mathcal{J}_-] = 2\mathcal{J}_0$, we could get

$$\begin{aligned}e^{x_-\mathcal{J}_-}\rho(t) &= (1+x_-\mathcal{J}_-)\rho(t), \\ e^{x_+\mathcal{J}_+}\rho(t) &= (1+x_+\mathcal{J}_+)\rho(t), \\ e^{(\ln x_0)\mathcal{J}_0}\rho(t) &= \rho(t) + (\sqrt{x_0}-1)P_0\rho(t)P_0 \\ &\quad + \left(\frac{1}{\sqrt{x_0}} - 1\right)P_1\rho(t)P_1,\end{aligned} \tag{A15}$$

where $P_0 = |\uparrow\rangle\langle\uparrow|$ and $P_1 = |\downarrow\rangle\langle\downarrow|$. Now we see the evolution of the projector $|\uparrow\rangle\langle\uparrow|$. By using Eq. (A15), after the

three actions, we obtain

$$e^{\frac{\gamma_0 t}{2}}\mathcal{V}(t)P_0 = \left(\sqrt{x_0} + \frac{x_+x_-}{\sqrt{x_0}}\right)|\uparrow\rangle\langle\uparrow| + \frac{x_-}{\sqrt{x_0}}|\downarrow\rangle\langle\downarrow|. \tag{A16}$$

Substituting the values of x_+, x_-, and x_0 given by Eq. (A14) into the above equation, we get

$$\mathcal{V}(t)P_0 = [1-\mathcal{G}(\alpha,\beta,t)]P_0 + \mathcal{G}(\alpha,\beta,t)P_1. \tag{A17}$$

This evolution operator can be further decomposed into three consecutive operators (see Appendix A), and finally we obtain

$$\begin{aligned}
&\mathcal{V}(t)(|\uparrow\rangle\langle\uparrow|) = [1-\mathcal{G}(\alpha,\beta,t)]|\uparrow\rangle\langle\uparrow| + \mathcal{G}(\alpha,\beta,t)|\downarrow\rangle\langle\downarrow|,\\
&\mathcal{V}(t)(|\downarrow\rangle\langle\downarrow|) = [1-\mathcal{G}(\beta,\alpha,t)]|\downarrow\rangle\langle\downarrow| + \mathcal{G}(\beta,\alpha,t)|\uparrow\rangle\langle\uparrow|,\\
&\mathcal{V}(t)(|\downarrow\rangle\langle\uparrow|) = e^{-\frac{1}{2}\gamma_0 t}|\downarrow\rangle\langle\uparrow|,\\
&\mathcal{V}(t)(|\uparrow\rangle\langle\downarrow|) = e^{-\frac{1}{2}\gamma_0 t}|\uparrow\rangle\langle\downarrow|,
\end{aligned} \tag{A18}$$

where the function

$$\mathcal{G}(\alpha,\beta,t) = \frac{\alpha(1-e^{-\gamma_0 t})}{\alpha+\beta}. \tag{A19}$$

By using Eq. (A19) and the explicit form of the initial density matrix in $|\uparrow\rangle\langle\uparrow|$, one obtains the density matrix at time t as

$$\begin{aligned}
\rho(t) = &\left[\cos^2\frac{\theta}{2}e^{-\gamma_0 t} + \mathcal{G}(\beta,\alpha,t)\right]|\uparrow\rangle\langle\uparrow|\\
&+ \frac{1}{2}e^{-i\phi}\sin\theta e^{-\frac{1}{2}\gamma_0 t}|\uparrow\rangle\langle\downarrow|\\
&+ \frac{1}{2}e^{i\phi}\sin\theta e^{-\frac{1}{2}\gamma_0 t}|\downarrow\rangle\langle\uparrow|\\
&+ \left[\sin^2\frac{\theta}{2}e^{-\gamma_0 t} + \mathcal{G}(\alpha,\beta,t)\right]|\downarrow\rangle\langle\downarrow|.
\end{aligned} \tag{A20}$$

We see that damping rate is two times of the dephasing rate, and this will lead to interesting behaviors of the reliability loss.

By direct calculation from Eq. (A20), the Bloch vector at the time t could be written as

$$\begin{aligned}
r_x(t) &= \sin\theta\cos\phi e^{-\frac{1}{2}\gamma_0 t},\\
r_y(t) &= \sin\theta\sin\phi e^{-\frac{1}{2}\gamma_0 t},\\
r_z(t) &= \cos\theta e^{-\gamma_0 t} + (1-2\bar{n})(e^{-\gamma_0 t}-1).
\end{aligned} \tag{A21}$$

By plugging the Bloch vector at $t_0 = 0$ and $t' = \delta t$ in Eq. (8), one has

$$\begin{aligned}
R(t) = \frac{1}{2^N}[&1 + \sin^2\theta e^{-\gamma_0 t/2N} + \cos^2\theta e^{-\gamma_0 t/N}\\
&+ (1-2\bar{n})\cos\theta(e^{-\gamma_0 t/N}-1)]^N.
\end{aligned} \tag{A22}$$

From this equation, we can obtain the expression for the quantum reliability of an atom initially in the excited state, with no photons in the excitation field ($\bar{n} = 0$ and $\theta = 0$ $\phi = 0$).

$$R(N\delta t) = e^{-\gamma_0 N\delta t}. \tag{A23}$$

As for the weights of different historical interferences, after a path becomes invalid at time $n\delta t$, the state changes from $|\uparrow\rangle\langle\uparrow|$ to $|\downarrow\rangle\langle\uparrow|$.Then, if the failure occurs at $m\delta t$ during the evolution, the projection result will become $\mathbb{1}|\downarrow\rangle\langle\uparrow|\uparrow\rangle\langle\downarrow|$. Therefore, the weights for all interference histories should be

$$\varrho_{NM} = 0. \tag{A24}$$

APPENDIX B: FIRST-ORDER COHERENCE FUNCTION REPRESENTATION OF THE OFF-DIAGONAL ELEMENTS

The quantized radiation field can invariably be separated into positive- and negative-frequency components:

$$\mathcal{E}(x,t) = \mathcal{E}^{(+)}(x,t) + \mathcal{E}^{(-)}(x,t), \tag{B1}$$

where, $\mathcal{E}^{(+)}(x,t) = \sum_k a_k e^{-i\omega_k t}e^{ikx}$ and $\mathcal{E}^{(-)}(x,t) = [\mathcal{E}^{(+)}(x,t)]^\dagger$.

When we detect the radiation field of the atom, it essentially corresponds to the process of absorbing photons from the field, that is, to the positive-frequency component of the radiation field. Assuming the initial state of the radiation field is $|i\rangle$ and the final state is $|j\rangle$, the transition probability from the initial to the final state can be expressed as:

$$|\langle j|\mathcal{E}^{(+)}(x,t)|i\rangle|^2. \tag{B2}$$

Since what we are concerned with is the detection outcome rather than the final state of the radiation field, we consider all possible final states:

$$\begin{aligned}
\sum_j |\langle j|\mathcal{E}^{(+)}(x,t)|i\rangle|^2 &= \langle i|\mathcal{E}^{(-)}(x,t)\sum_j |j\rangle\langle j|\mathcal{E}^{(+)}(x,t)|i\rangle\\
&= \langle i|\mathcal{E}^{(-)}(x,t)\mathcal{E}^{(+)}(x,t)|i\rangle,
\end{aligned} \tag{B3}$$

where, we consider the completeness condition $\sum_j |j\rangle\langle j| = \mathbb{1}$.

Since the initial state of the atomic radiation field is represented by $|\psi(\delta t)\rangle$, and the two radiation fields are identical and emitted at the same position with a time delay of $(M-N)\delta t$, then the quantized radiation field operator can be written as

$$\mathcal{E}^{(+)}(x,t) = \mathcal{E}^{(+)}(x,t) + \mathcal{E}^{(+)}(x,t+(M-N)\delta t). \tag{B4}$$

Consequently, the measurable intensity of the radiation field is given by

$$\begin{aligned}
I(x,t) &= \langle\psi(\delta t)|[\mathcal{E}^{(-)}(x,t) + \mathcal{E}^{(-)}(x,t+(M-N)\delta t)][\mathcal{E}^{(+)}(x,t) + \mathcal{E}^{(+)}(x,t+(M-N)\delta t)]|\psi(\delta t)\rangle\\
&= \langle\psi(\delta t)|\mathcal{E}^{(-)}(x,t)\mathcal{E}^{(+)}(x,t)|\psi(\delta t)\rangle + \langle\psi(\delta t)|\mathcal{E}^{(-)}(x,t+(M-N)\delta t)\mathcal{E}^{(+)}(x,t+(M-N)\delta t)|\psi(\delta t)\rangle\\
&\quad + 2\mathrm{Re}(\langle\psi(\delta t)|\mathcal{E}^{(-)}(x,t)\mathcal{E}^{(+)}(x,t+(M-N)\delta t)|\psi(\delta t)\rangle)\\
&= G^{(1)}_{\delta t}(x,x;t,t) + G^{(1)}_{\delta t}(x,x;t+(M-N)\delta t, t+(M-N)\delta t) + 2G^{(1)}_{\delta t}(x,x;t,t+(M-N)\delta t).
\end{aligned} \tag{B5}$$

where, $G^{(1)}_{\delta t}(x,x;t,t')$ denotes the first-order correlation function; the first two terms in the above expression represent the individual intensities of the two radiation fields, while the third term corresponds to the interference between them.

Next, based on the definition of the off-diagonal elements, they can be expressed as

$$\varrho_{NM} = b^{(N-1)}(\delta t)b^{*(M-1)}(\delta t) \times \langle\psi_0|U^{\dagger}(\delta t)E_0^{\perp}U((M-N)\delta t)E_0^{\perp}U(\delta t)|\psi_0\rangle = b^{(N-1)}(\delta t)b^{*(M-1)}(\delta t)\mathcal{F}((M-N)\delta t), \tag{B6}$$

where, $\mathcal{F}((M-N)\delta t)$ can be expressed as

$$\begin{aligned}
\mathcal{F}((M-N)\delta t) &= \langle\psi_0|\, U_M^{\dagger}(\delta t)E_0^{\perp}U((M-N)\delta t)E_0^{\perp}U_N(\delta t)\,|\psi_0\rangle \\
&= \langle\psi(\delta t)|\, E_0^{\perp}U((M-N)\delta t)E_0^{\perp}\,|\psi(\delta t)\rangle \\
&\approx \langle\psi(\delta t)|\sum_{k'} a_{k'}^{\dagger}\sum_{k} a_k e^{-\mathrm{i}\omega_k(M-N)\delta t}\,|\psi(\delta t)\rangle \\
&= \int_{-\infty}^{\infty}\mathrm{d}x\,\langle\psi(\delta t)|\sum_{k} a_k^{\dagger}e^{-\mathrm{i}kx}\sum_{k} e^{-\mathrm{i}\omega_k(M-N)\delta t}e^{\mathrm{i}kx}a_k\,|\psi(\delta t)\rangle \\
&= \int_{-\infty}^{\infty}\mathrm{d}x\,\langle\psi(\delta t)|\,\mathcal{E}^{(-)}(x,0)\mathcal{E}^{(+)}(x,(M-N)\delta t)\,|\psi(\delta t)\rangle \\
&= \int_{-\infty}^{\infty}\mathrm{d}x G^{(1)}_{\delta t}(x,x;(M-N)\delta t,0),
\end{aligned} \tag{B7}$$

where, the off-diagonal elements represent interference between different histories, and only the temporal effect is relevant, an integration over the entire space is performed. Therefore, the off-diagonal elements can be associated with the first-order correlation function.

[1] M. Rausand and A. Høyland, *System Reliability Theory: Models, Statistical Methods, and Applicatoins* (John Wiley & Sons, New York, 2004).

[2] E. T. Jaynes, Information theory and statistical mechanics, Phys. Rev. **106**, 620 (1957).

[3] E. T. Jaynes, Information theory and statistical mechanics II, Phys. Rev. **108**, 171 (1957).

[4] Y.-M. Du, Y. H. Ma, Y. F. Wei, X. F. Guan, and C. P. Sun, Maximum entropy approach to reliability, Phys. Rev. E **101**, 012106 (2020).

[5] Y-M. Du and C. P. Sun, A novel interpretable model of bathtub hazard rate based on system hierarchy, Reliab. Eng. Syst. Safe. **228**, 108756 (2022).

[6] L. X. Cui, Y-M. Du, and C. P. Sun, Quantum reliability, Phys. Rev. Lett. **131**, 160203 (2023).

[7] R. B. Griffiths, *Consistent Quantum Theory* (Cambridge University Press, New York, 2001).

[8] M. A. Nielsen and I. L. Chuang, *Quantum Computation and Quantum Information* (Cambridge University Press, Cambridge, England, 2000).

[9] B. M. Terhal, Quantum error correction for quantum memories, Rev. Mod. Phys. **87**, 307 (2015).

[10] P. Rocchi, *Reliability is a New Science* (Springer International Publishing, Berlin, 2017).

[11] L.-X. Cui, Y.-M. Du, and C. P. Sun, On quantum reliability characterizing systematic errors in quantum sensing, J. Reliab. Sci. Eng. **1**, 015004 (2025).

[12] C. L. Degen, F. Reinhard, and P. Cappellaro, Quantum sensing, Rev. Mod. Phys. **89**, 035002 (2017).

[13] G. Wendin, Quantum information processing with superconducting circuits: A review, Rep. Prog. Phys. **80**, 106001 (2017).

[14] M. Fleischhauer, M. D. Lukin, Quantum memory for photons: Dark-state polaritons, Phys. Rev. A **65**, 022314 (2002).

[15] E. Altman, K. Brown, G. Carleo, L. Carr, E. Demler, C. Chin *et al.*, Quantum simulators: Architectures and opportunities, PRX Quantum **2**, 017003 (2021).

[16] A. Uhlmann, The "transition probability" in the state space of a ∗-algebra, Rep. Math. Phys. **9**, 273 (1976).

[17] P. E. M. F. Mendonça, R. J. Napolitano, M. A. Marchiolli, C. J. Foster, and Y. C. Liang, Alternative fidelity measure between quantum states, Phys. Rev. A **78**, 052330 (2008).

[18] X. Wang, C. S. Yu, and X. X. Yi, An alternative quantum fidelity for mixed states of qudits, Phys. Lett. A **373**, 58 (2008).

[19] J. Liu, X. M. Lu, J. Ma, and X. Wang, Fidelity and fidelity susceptibility based on Hilbert-Schmidt inner product, Sci. China Phys. Mech. Astron. **55**, 1529 (2012).

[20] J. L. Chen, L. B. Fu, A. A. Ungar, and X. G. Zhao, Alternative fidelity measure between two states of an n-state quantum system, Phys. Rev. A **65**, 054304 (2002)

[21] D. J. C. Bures, An extension of Kakutani's theorem on infinite product measures to the tensor product of semifinite w*-algebras, Trans. Am Math. Soc. **135**, 199 (1969).

[22] H. P., Breuer, F. Petruccione, *The Theory of Open Quantum Systems* (Oxford University Press, New York, 2002).

[23] L. H. Pedersen, N. M. Møller, and K. Mølmer, Fidelity of quantum operations, Phys. Lett. A **367**, 47 (2007).

[24] H. Friedman, D. A. Kessler and E. Barkai, Quantum walks: The first detected passage time problem, Phys. Rev. E **95**, 032141 (2017).

[25] J. G. Muga, R. Sala Mayato, and Í. L. Egusquiza, *Time in Quantum Mechanics* (Springer, Berlin, Heidelberg, 2008).

[26] H. E. Hauge and J. A. Støvneng, Tunneling times: A critical review, Rev. Mod. Phys. **61**, 917 (1989).

[27] A. M. Steinberg, Time and history in quantum tunneling, Superlattices Microstruct. **23**, 823 (1998).
[28] S. Yusofsani and M. Kolesik, Quantum tunneling time: Insights from an exactly solvable model, Phys. Rev. A **101**, 052121 (2020).
[29] L. J. Jia, L. Xu, P. Zhang, and L. B. Fu, Effects of time on the evolution of a wave packet in the tunneling dynamics, New J. Phys. **23**, 113047 (2021).
[30] L. J. Jia, H. J. Xing, and L. B. Fu, Larmor time of a bound electron wave packet tunneling through a barrier, Phys. Rev. A **105**, 062804 (2022).
[31] T. Petrosky, G. Ordonez, and I. Prigogine, Space-time formulation of quantum transitions, Phys. Rev. A **64**, 062101 (2001).
[32] U. M. Titulaer, R. J. Glauber, Correlation functions for coherent fields, Phys. Rev. **140**, B676 (1965).
[33] R. B. Griffiths, Consistent histories and the interpretation of quantum mechanics, J. Stat. Phys. **36**, 219 (1984).
[34] Y. Aharonov, and D. Bohm, Time in the quantum theory and the uncertainty relation for time and energy, Phys. Rev. **122**, 1649 (1961).
[35] M. Fadel, L. Maccone, Time-energy uncertainty relation for quantum events, Phys. Rev. A **104**, L050204 (2021).
[36] Y. T. Li, Y.-M. Du, W. K. Ding, Z. Y. Fei, L. B. Fu, and X. G. Wang, Numerical data underlying figures in "Constructing the nonclassical lifetime distribution of two-level systems via quantum reliability" (version v1), Zenodo (2025), https://zenodo.org/records/16888743.

Correction: A grant number in the Acknowledgments contained an error and has been fixed.